PHYSICAL REVIEW B VOLUME 45, NUMBER 23 15 JUNE 1992-I

Structural and electronic properties of metastable epitaxial $FeSi_{1+x}$ films on Si(111)

H. von Känel, K. A. Mäder, E. Müller, N. Onda, and H. Sirringhaus
Laboratorium für Festkörperphysik, Eidgenössische Technische Hochschule Hönggerberg, CH-8093 Zürich, Switzerland
(Received 5 March 1992)

We have investigated the epitaxial growth and the electronic properties of a metallic metastable FeSi phase crystallizing with the CsCl structure on Si(111). Upon annealing below 500 °C the stoichiometry of thin films (< 20 Å) evolves towards $FeSi_2$ with no change of symmetry, i.e., the defect CsCl structure with a statistical occupation of metal sites remains epitaxially stable for all $FeSi_{1+x}$ ($0 \leq x \leq 1$). Films thicker than ~ 20 Å exhibit a transition to the cubic ϵ-FeSi phase. The electronic band structure of FeSi (CsCl) has been calculated self-consistently using the full-potential linear augmented-plane-wave method.

The epitaxial growth of an overlayer whose lattice constant a_l deviates little from the substrate lattice constant a_0 is well under control experimentally and well understood theoretically. For a misfit $f=(a_l-a_0)/a_0$ of typically a few percent one expects an epitaxial film to grow coherently, i.e., homogeneously strained with its lateral lattice parameter $a_\parallel$ perfectly matched to a_0. At some critical thickness h_c the strain energy stored in the film becomes too large and coherency breaks down due to the formation of misfit dislocations.[1,2] While the calculations of critical layer thickness for systems with small misfit make explicit use of linear elasticity theory,[1,2] this is no longer justified for misfits above, say 10%. The overlayer may then adopt a crystal structure which is lattice matched well to the substrate but which differs from the usual bulk form. Examples of such systems are α-Sn deposited on InSb or CdTe (Ref. 3) and bcc Co on GaAs.[4] The theory for such structural changes in epitaxial overlayers was developed in Ref. 5.

In this paper we report on the successful synthesis of FeSi with the metastable CsCl structure by molecular-beam epitaxy (MBE). The corresponding bulk phase, ϵ-FeSi, of this material is simple cubic and has a lattice constant of 4.4 Å (Ref. 6) to be compared with the Si lattice parameter of 5.43 Å. This latter phase also was previously found to grow epitaxially on Si(111) with (111) ϵ-FeSi$\parallel$(111) Si and $\langle 0\bar{1}1\rangle$FeSi$\parallel\langle\bar{2}11\rangle$ Si.[7] For these crystallographic directions the mismatch amounts to $f=-6.4\%$ at room temperature (RT). The geometric mismatch is not, however, the only factor relevant to epitaxy. The atomic arrangements in the (111) plane of ϵ-FeSi and of Si are vastly different. We hence have to expect the interfacial energy to be significantly greater for this epitaxial couple than for the simple overlayer/substrate couple we are going to discuss.

FeSi was grown on clean (111) Si 7×7 substrates (n doped, 1–2000 Ω cm) with parallel monolayer steps due to the unintentional misorientation of 0.1–0.3°. Details of the substrate preparation procedure can be found in Ref. 8.

The silicide was grown at RT (< 100 °C) by depositing 2 monolayers (ML) of pure Fe followed by the codeposition of Fe and Si at a stoichiometric ratio (1:1) until the desired thickness of 5–80 Å was reached. The 1×1 reflection high-energy electron-diffraction (RHEED) pattern exhibited well-defined Kikuchi bands of cubic symmetry. The orientation of the epitaxial FeSi films was always of type B, i.e., with respect to the substrate the overlayer is rotated by 180° around the surface normal. The analysis of the Kikuchi pattern as well as transmission electron-diffraction patterns showed that this FeSi phase has the simple cubic CsCl structure with a lattice parameter close to half the Si lattice constant. The same observation has been made by Smilgies and Robinson by their x-ray truncation rod technique.[9] When the CsCl diffraction spots are indexed according to a cubic cell with the Si-cell parameter, all (hkl) reflections with odd indices are absent [Fig. 1(a)]. By contrast, in the diffraction patterns of γ-$FeSi_2$ (Ref. 10) and $CoSi_2$ both having the fluorite structure these spots are always present [Figs. 1(b) and 1(c)]. The contrast of high-resolution images of FeSi also differs strongly from that of γ-$FeSi_2$ and $CoSi_2$ [Figs. 1(d)–1(f)]. The inferior quality of micrographs showing the FeSi phase is due to magnetic effects present at the surface of these silicide layers.

The surface structure of FeSi was investigated by *in situ* scanning tunneling microscopy (STM). After the RT deposition of the silicide the surface morphology was found to reflect closely the step structure present before on the bare Si surface. The STM topograph shown in Fig. 2(a) stems from a FeSi film of 25 Å thickness. Only misorientation-induced surface steps of 3.1 Å height are present, clearly indicating layer-by-layer growth. This growth mode is maintained up to film thicknesses of at least 50 Å. Although the Kikuchi bands were rather sharp after RT deposition, the surface was found to be disordered on an atomic scale. STM topographs revealed a grainy structure with a roughness of 1–2 Å.

The ultraviolet photoemission spectroscopy (UPS) valence-band spectra (Fig. 3, curve a) show a distinct Fermi edge, indicating that this phase is metallic. Typical for these spectra are two peaks situated at 0.4 and 0.8 eV. Within the resolution of our UPS spectrometer (0.1 eV) these density of states (DOS) features were present in all FeSi layers independent of their thickness. Therefore these valence-band spectra represent a clear fingerprint of this phase.

Upon annealing, the valence structure and the crystal

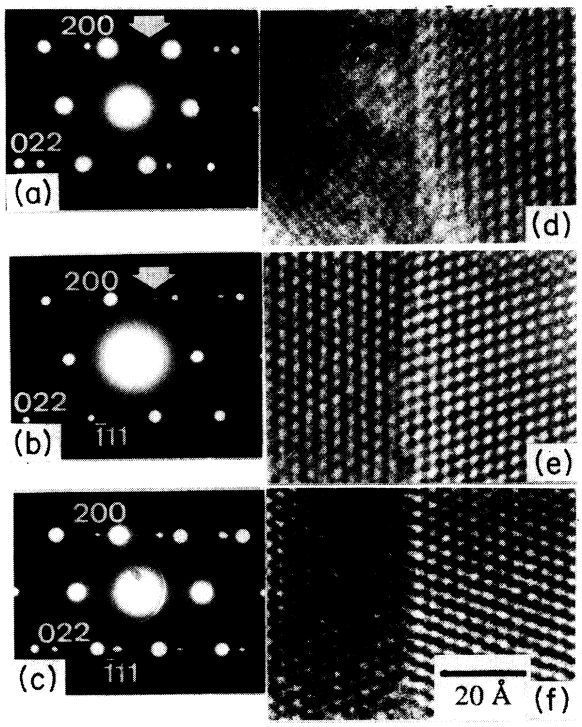

FIG. 1. The diffraction patterns of (a) FeSi (CsCl structure), (b) γ-$FeSi_2$ (CaF_2 structure), and (c) $CoSi_2$ (CaF_2 structure) on Si(111) are taken along the $[0\bar{1}1]$ direction. Only silicide spots (for a cubic cell with the Si-cell parameter) are indexed. The corresponding high-resolution images are also given along the $[0\bar{1}1]$ direction: (d) FeSi on Si, (e) γ-$FeSi_2$ on Si, and (f) $CoSi_2$ on Si.

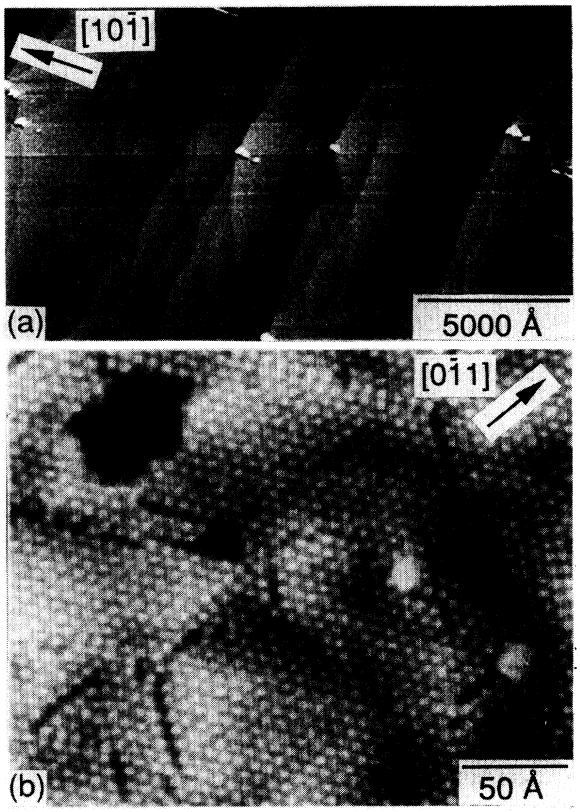

FIG. 2. STM greyscale topographs of (a) 25-Å FeSi after RT deposition (empty state image obtained with a tunneling voltage $V_T = 2$ V and a tunneling current $I_T = 1$ nA). (b) 8-Å FeSi after annealing at 500 °C ($V_T = 2$ V, $I_T = 0.5$ nA). In (b) the hole in the upper left, which appears black for reasons of contrast enhancement, was 1.6 Å deep, the 2×2 reconstruction resolved on the bottom level was indistinguishable from the one on the top level.

structure develop in two completely different ways depending on the initial thickness of the epitaxial film. We will treat these two cases separately.

Films thinner than ~15 Å remain metallic up to a critical temperature of about 550–650 °C where they undergo an irreversible phase transition to semiconducting β-$FeSi_2$. During the annealing process a continuous increase of the Si content takes place. The analysis of Fe $2p$ and Si $2p$ x-ray photoemission spectroscopy core-level intensities reveals that the stoichiometry changes from FeSi to $FeSi_2$. TEM cross sections support this finding, showing a clear increase of the film thickness compared to the as-deposited one. It is important to emphasize that the symmetry of the phase does not change during the annealing process. We find the same diffraction pattern as that in Fig. 1(a), indicating that the structure of $FeSi_{1+x}$ ($0 \leq x \leq 1$) can be derived from the CsCl structure by introducing Fe vacancies distributed in a random fashion. By comparing Figs. 1(a) and 1(b) it becomes obvious that $FeSi_{1+x}$ with such a defect CsCl structure can be well distinguished from the γ-$FeSi_2$ phase. The latter develops only upon prolonged annealing close to the transition to the β-$FeSi_2$ phase.

The surface structure changes also during the annealing process. Depending on film thickness a 2×2 reconstructed phase appears around 300–350 °C as evidenced by RHEED and STM. As an example Fig. 2(b) shows an STM topograph of FeSi after annealing to 500 °C. The as-deposited film thickness was 8 Å in this case. The mean size of the 2×2 reconstructed domains is ~100 ×100 $Å^2$. Several domain boundaries are visible in Fig. 2(b). The surface step height has changed from 3.1 to 1.6 Å. STM topographs and spectroscopy did not reveal any significant differences between adjacent terraces separated by a surface step. This requires the distance between equivalent atomic planes to be half as large as in the CaF_2 structure in accordance with the TEM results indicating CsCl symmetry. Films grown intentionally with a stoichiometry of 1:2 exhibited the same surface structure. The slight corrugation visible on a 100-Å scale in Fig. 2(b) will be discussed in more detail in a forthcoming publication.

The valence-band spectrum of a 10-Å-thick FeSi film after annealing to 550 °C is displayed in Fig. 3 (curve *b*). The main peak has shifted slightly towards higher binding energy, while the one at 0.4 eV (curve *a*) is entirely absent. The Fermi edge persists, but it is smaller by a factor of ~4 compared to the unannealed film. Both the valence-band spectra and the RHEED patterns of annealed FeSi films fit very well the corresponding ones ob-

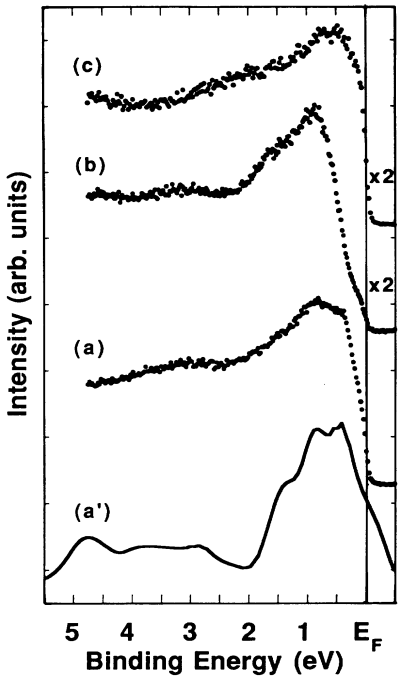

FIG. 3. UPS spectra taken with He I radiation ($h\nu$=21.2 eV) on (a) a 10-Å-thick $FeSi_2$ film grown at RT, (b) the same film after annealing to 550 °C, (c) a 30-Å film which has undergone the phase transition to the ϵ-FeSi phase due to annealing to 400 °C, and (a') theoretical DOS of FeSi (CsCl), shifted to lower binding energies by 1.2 eV.

tained on films grown by coevaporation of Fe and Si on Si(111) in the ratio 1:2.[10]

FeSi films with thicknesses larger than ~20 Å behave very differently upon annealing. As mentioned above for as-grown samples, both the RHEED pattern and the valence-band spectra do not depend on the thickness of the films. For a 30-Å film the 1×1 RHEED pattern disappears abruptly near 300 °C. The valence-band spectrum of this "disordered" phase is displayed in Fig. 3 (curve *c*). It is characterized by a main peak situated at 0.6 eV and a large Fermi edge. Similar UPS spectra have been found by Alvarez *et al.*[11] on single-crystal ϵ-FeSi. Our TEM analysis on films which have undergone the phase transition reveals indeed the presence of heavily twinned ϵ-FeSi. A detailed account of phase transitions in epitaxial $FeSi_{1+x}$ films will be given elsewhere.

We have calculated the electronic band structure of the ordered end members of the series $FeSi_{1+x}$ ($0 \le x \le 1$), i.e., FeSi and γ-$FeSi_2$ (Ref. 10) self-consistently using the full-potential linear augmented-plane-wave (FLAPW) method. Up to 50 APW's per atom were included in the basis set, and the irreducible wedge of the Brillouin zone was sampled over 32 and 80 **k** points for total energy and DOS calculations, respectively. Self-consistent runs with higher cutoffs revealed no change in the band structure. Inside the muffin-tin spheres spherical harmonics with angular momentum up to $L_{max}=8$ were included.

The band structure and DOS (Ref. 10) of γ-$FeSi_2$ agrees very well with an LMTO calculation of Christensen.[12] In this paper we focus on the properties of the CsCl phase of FeSi and compare them with the known results on γ-$FeSi_2$.

Minimizing the total energy yields an equilibrium lattice constant for FeSi of $a_1=2.717$ Å, and a bulk modulus $B_0=2.63$ Mbar. Lattice constants tend to be underestimated by FLAPW by at most 3%. We thus expect FeSi to be under compressive strain since $2a_1 > a_{Si}$. This is indeed confirmed experimentally by transmission electron microscopy and by Rutherford backscattering.

The Fe-Si distance is virtually the same in FeSi and γ-$FeSi_2$. In the CsCl structure Si has eight nearest neighbors (four in the fluorite structure), whereas the local environment of Fe is the same for the two crystal lattices (eight Si *nn*). The partial Si *s* and *p* DOS of the two structures are very similar and show an overlap as in $CoSi_2$.[13] In the CsCl structure, however, sp^3 hybridization cannot be anticipated, since the point symmetry at the Si site is O_h. The Si *p* orbitals thus transform like Γ_{15}, whereas in the fluorite structure there are six Si *p* orbitals that form bonding $\Gamma_{25'}$ and antibonding Γ_{15} linear combinations. Hence in γ-$FeSi_2$ these $\Gamma_{25'}$ states hybridize with the Fe *d* orbitals of the same symmetry (*xy*, *yz*, and *xz*), whereupon the latter lower their energy with respect to the nonbonding *d* orbitals of Γ_{12} symmetry. This is basically the picture proposed by Tersoff and Hamann for the bonding in $CoSi_2$ and $NiSi_2$.[13] Indeed, for γ-$FeSi_2$ the self-consistent charge redistribution due to the crystal potential shows a weak accumulation in the Fe-Si bond region with respect to the superposition of the atomic charges. In FeSi, on the other hand, we do not observe an important "covalent" contribution to the charge density. The material is rather polar due to an accumulation of electronic charge at the Fe sites.[14] Furthermore, we note that in FeSi the band order is reversed, i.e., Γ_{12} is below $\Gamma_{25'}$ (see Fig. 4). This is consistent with the crystal field splitting of *d* states expected due to the charge transfer. The *d*-*d* interaction between nearest Fe neighbors further enhances the Γ_{12}-$\Gamma_{25'}$ splitting to a total of ~3 eV. This is

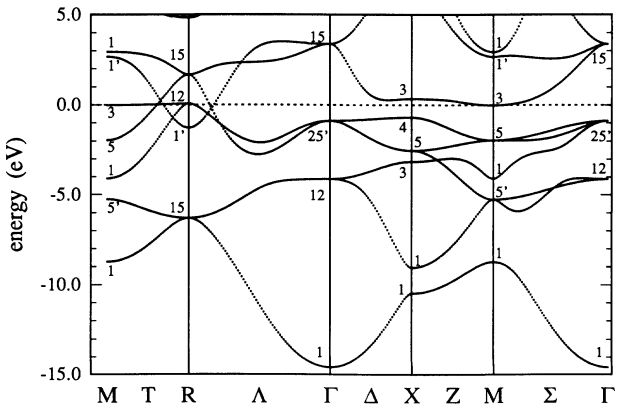

FIG. 4. Energy-band dispersion of FeSi in the CsCl structure as obtained by the FLAPW calculation within the local-density approximation. Note the reversed band order of the Fe *d* states at Γ as compared to γ-$FeSi_2$ (Ref. 12). The Si *p*-like states are found at the *R* point (R_{15}).

rather large as compared to other transition metal silicides. Returning to the band structure of FeSi (Fig. 4) we see that the main DOS features (Fig. 3, curve a') are derived from the d bands with peaks attributed to $\Gamma_{25'}$, $M_{5'}$, X_5, and Γ_{12}. The Si p-like R_{15} states, located at 6 eV below E_F, are not discernible in experimental spectra covering this energy range. The theoretical DOS has been rigidly shifted by 1.2 eV towards the Fermi level for better comparison with the experimental spectrum (curve a). In reality it is the experimental d-band features which appear at unusually low binding energies due to intra-atomic relaxation effects.[14,15] The shape of the main DOS peak agrees well with the UPS data. At higher binding energies secondary electrons contribute significantly to the measured spectra, and thus the relative intensity of the UPS peak at 3 eV appears higher than the corresponding DOS feature, which we attribute to Γ_{12} states.

In summary, we have given the first account of an epitaxial FeSi phase crystallizing with the CsCl structure. By annealing thin films of this material its composition can continuously be changed towards $FeSi_2$ with no change of symmetry.

The authors wish to express their deep appreciation to A. Baldereschi, R. Monnier, and H.-U. Nissen for valuable discussions and to M. Posternak for the permission to use his FLAPW code. Special thanks are due to D.-M. Smilgies and I. K. Robinson for communicating their results on x-ray interference prior to publication. Financial support by the Swiss National Science Foundation is also gratefully acknowledged.

[1]J. H. van der Merwe, Surf. Sci. **31**, 198 (1972).

[2]J. W. Matthews and A. E. Blakeslee, J. Cryst. Growth **27**, 118 (1974).

[3]R. F. C. Farrow, D. S. Robertson, G. M. Williams, A. G. Cullis, G. R. Jones, I. M. Young, and P. N. J. Dennis, J. Cryst. Growth **54**, 507 (1981).

[4]G. A. Prinz, Phys. Rev. Lett. **54**, 1051 (1985).

[5]R. Bruinsma and A. Zangwill, J. Phys. (Paris) **47**, 2055 (1986).

[6]H. Watanabe, H. Yamamoto, and Ken-ichi Ho, J. Phys. Soc. Jpn. **18**, 995 (1963).

[7]J. Chevrier, V. Le Thanh, S. Nitsche, and J. Derrien, Appl. Surf. Sci. **56–58**, 438 (1992).

[8]H. von Känel, R. Stalder, H. Sirringhaus, N. Onda, and J. Henz, Appl. Surf. Sci. **53**, 196 (1991).

[9]D.-M. Smilgies and I. K. Robinson (private communication).

[10]N. Onda, J. Henz, E. Müller, K. A. Mäder, and H. von Känel, Appl Surf. Sci. **56–58**, 421 (1992); N. Onda, J. Henz, E. Müller, H. von Känel, C. Schwarz, and R. E. Pixley, Helv. Phys. Acta **64**, 197 (1991).

[11]J. Alvarez, J. J. Hinarejos, E. G. Michel, G. R. Castro, and R. Miranda (unpublished).

[12]N. E. Christensen, Phys. Rev. B **42**, 7148 (1990).

[13]J. Tersoff and D. R. Hamann, Phys. Rev. B **28**, 1168 (1983).

[14]In FeSi the transfer of -0.5 electronic charges per unit cell to d orbitals localized within the Fe muffin-tin sphere leads to a partial ionic character of this material. This charge distribution enhances the stability of the CsCl structure by contributing a Madelung term to the total energy. On the other hand, the strong charge localization at the Fe sites must be expected to lead to unusually large intra-atomic relaxation effects in valence-band photoemission. For free Fe atoms intra-atomic relaxation amounts to 3.8 eV (see Ref. 15). This is sufficient to explain qualitatively the shift of the experimental spectrum (Fig. 3, curve a) to lower binding energy by 1.2 eV.

[15]U. Gelius and K. Siegbahn, Institute of Physics, Uppsala University Report No. UU IP-794, 1972.

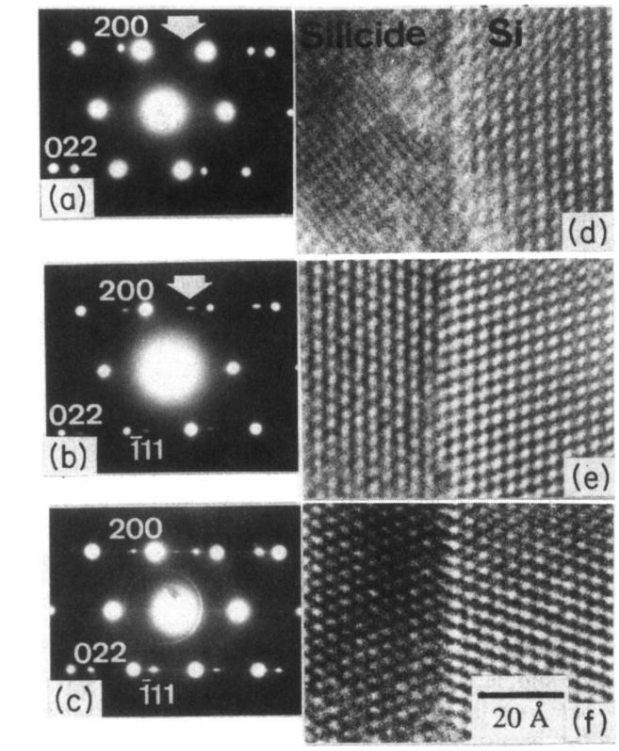

FIG. 1. The diffraction patterns of (a) FeSi (CsCl structure), (b) γ-$FeSi_2$ (CaF_2 structure), and (c) $CoSi_2$ (CaF_2 structure) on Si(111) are taken along the $[0\bar{1}1]$ direction. Only silicide spots (for a cubic cell with the Si-cell parameter) are indexed. The corresponding high-resolution images are also given along the $[0\bar{1}1]$ direction: (d) FeSi on Si, (e) γ-$FeSi_2$ on Si, and (f) $CoSi_2$ on Si.

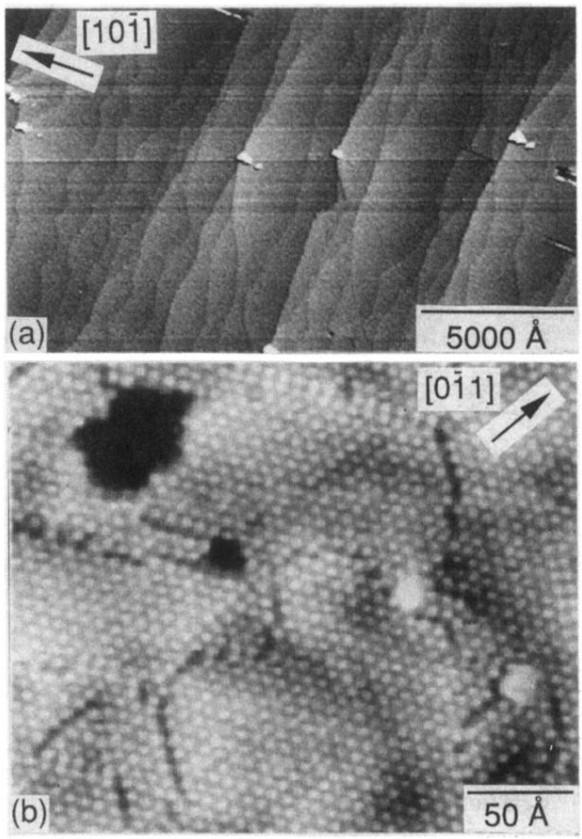

FIG. 2. STM greyscale topographs of (a) 25-Å FeSi after RT deposition (empty state image obtained with a tunneling voltage $V_T = 2$ V and a tunneling current $I_T = 1$ nA). (b) 8-Å FeSi after annealing at 500 °C ($V_T = 2$ V, $I_T = 0.5$ nA). In (b) the hole in the upper left, which appears black for reasons of contrast enhancement, was 1.6 Å deep, the 2×2 reconstruction resolved on the bottom level was indistinguishable from the one on the top level.